Optical properties of hybrid quantum dot/quantum well active region based on GaAs system

Jiri Thoma, Tomasz J. Ochalski, Maxime Hugues, Shiyong Zhang, Stephen P. Hegarty, and Guillaume Huyet

Citation: Journal of Applied Physics **112**, 063103 (2012); doi: 10.1063/1.4752279
View online: http://dx.doi.org/10.1063/1.4752279
View Table of Contents: http://aip.scitation.org/toc/jap/112/6
Published by the American Institute of Physics

Optical properties of hybrid quantum dot/quantum well active region based on GaAs system

Jiri Thoma,[1,2] Tomasz J. Ochalski,[1,2] Maxime Hugues,[3] Shiyong Zhang,[3] Stephen P. Hegarty,[2] and Guillaume Huyet[1,2]
[1]*Centre for Advanced Photonics & Process Analysis, Cork Institute of Technology, Ireland*
[2]*Tyndall National Institute, UCC, Lee Maltings, Cork, Ireland*
[3]*Department of Electronic and Electrical Engineering, University of Sheffield, Mappin Street, Sheffield S1 4JD, United Kingdom*

(Received 28 June 2012; accepted 9 August 2012; published online 17 September 2012)

We experimentally investigate the optical properties of a novel hybrid material/structure consisting of a GaInNAs quantum well and stacked InAs/InGaAs quantum dot layers on GaAs substrate. We demonstrate that the strong quantum confined Stark effect within the quantum well can effectively control well-dot detuning when reverse bias voltage is applied. With a combination of low- and room-temperature time resolved luminescence spectra we infer device absorption recovery time under 30 ps. These properties could be utilized in high-speed optoelectronics devices, in particular electro-absorption modulated lasers and reconfigurable multisection devices, where the hybrid quantum dots – quantum well material system could offer easily and rapidly interchangeable function, i.e., emission gain or variable attenuation, of each section depending on the external bias.
 [http://dx.doi.org/10.1063/1.4752279]

Since their proposal, semiconductor quantum dots (QDs) grown on GaAs substrates have been intensively investigated due to their distinct optoelectronic properties when compared with quantum well (QW) devices.[1] Low threshold current density ($<12\,A/cm^2$),[2] high temperature stability ($T_0 > 650$ K)[3] and low relative intensity noise ($-158\,dB/Hz$)[4] have been demonstrated. Multi-section monolithic mode-locked QD lasers have shown pulse-widths as low as 400 fs,[5] with repetition rates over 200 GHz.[6] Despite the excellent performance, QD lasers have also shown modest maximum modulation bandwidths, a weak quantum confined Stark effect (QCSE) and low absorption.[7] This makes high-speed integrated electro-absorption modulated lasers (EMLs) impractical. One of possible ways to improve QD device performance is by growing a hybrid material system combining both QDs and QWs. The tunnel injection structure is an example, where electronic coupling between a QW and a QD layer can improve carrier transfer to the QD ground state.[8,9] To match the telecommunication window, a large interest has been dedicated to the optimization of QDs emitting at 1.3 μm on GaAs. This choice of substrate and wavelength however greatly limits the choice of QW material if lattice matching is to be achieved. For QW emission at this wavelength, the most serious candidate is the quaternary GaInNAs (GINA) alloy, where a low percentage of nitrogen incorporation can lead to a rapid reduction in bandgap energy. The development of the GINA system has been spurred on by its large conduction band offset with respect to GaAs, reducing thermal escape of carriers and allowing high temperature uncooled operation[10] while still offering sufficiently high modal gain.[11] In addition, this material (particularly when annealed) exhibits a QCSE with exciton shift >40 nm (34 meV) and absorption coefficient $>6000\,cm^{-1}$ at electric field of 70 kV/cm.[12] To take advantage of these electro-absorption properties in a biased monolithic device will require the fabrication of multi-contacted devices, however many of the integration approaches (butt-coupling, selected area growth, etc.,) suffer from challenging growth and/or fabrication requirements.[13] One possible way to ease such device integration lies in stacking all the structures on top of each other, sharing an identical active region (IAR) within an optical waveguide. Except the simplified device manufacturing the stacking could be utilized in fast reconfigurable multisection devices[14] where each section could play different role, i.e., either provides emission gain or variable attenuation, in overall device design depending on the external bias applied.

In this work, we have grown and experimentally studied a set of wafers grown by molecular beam epitaxy (MBE) on n++ GaAs substrate using a VG Semicon V80 system. The hybrid p-i-n sample consists of six stacked InAs/$In_{0.15}Ga_{0.85}$As/GaAs dots-in-well (DWELL) layers and one $Ga_{0.65}In_{0.35}N_{0.015}As_{0.985}$/GaAs 6 nm (GINA) QW [Fig. 1]. First, in order to prevent any electronic coupling, the QD and QW layers were separated by 125 nm of GaAs. Second, to prevent any strain propagation and dislocation between QD layers, the consecutive QD layers were separated by 45 nm spacer layers consisting of 5 nm low temperature grown (520 °C) GaAs and 40 nm high temperature grown (580 °C) GaAs.[15] The intrinsic layers are situated inside an IAR delimited by a mixture of 50 nm and 100 nm upper (p-doped) and lower (n-doped) $Al_{0.3}Ga_{0.7}As$ cladding layers with concentration of $5 \times 10^{17}\,cm^{-3}$ and $1 \times 10^{18}\,cm^{-3}$ Silicon for the n-doped lower cladding and $5 \times 10^{17}\,cm^{-3}$ and $2 \times 10^{18}\,cm^{-3}$ Beryllium for the p-doped upper cladding, respectively. To study the electro-absorption performance of both the dilute-nitride QW and the QD layers, the p-i-n sample was processed into a set of mesas with inner diameter of 20 μm and metal contacts applied. To evaluate and identify all the features within

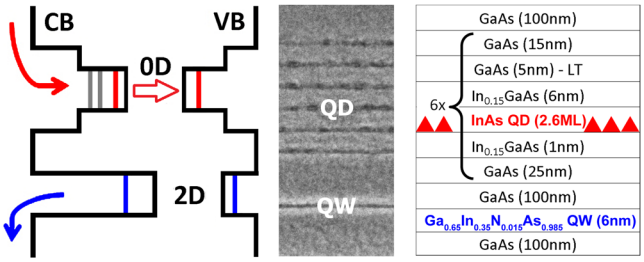

FIG. 1. The band structure of the proposed hybrid structure material consisting of six InAs DWELL layers and GINA QW on n++ GaAs substrate together with cross-sectional transmission electron microscopy image of the active region and with detailed active region composition of the hybrid p-i-n sample.

the hybrid p-i-n sample, both a single $Ga_{0.63}In_{0.37}N_{0.015}As_{0.985}$/GaAs 6 nm QW and six stacked InAs/$In_{0.15}Ga_{0.85}As$/GaAs DWELL intrinsic samples have been grown separately as well.

Room temperature (RT) photoluminescence (PL) measurements (confocal geometry, Ti:Sapphire 800 nm excitation laser) of the QD sample [Fig. 2(a)] showed a ground state (GS) emission at 1310 nm and a first excited state (1ES) emission peak at 1210 nm while for the QW sample the emission peak is centred at 1260 nm. RT PL spectra of the p-i-n sample were dominated by QD features with no clear contribution from the QW. This is interpreted as a consequence of the large nonradiative recombination centers (NRR) density inside the GINA QW and the growth geometry as the QW is

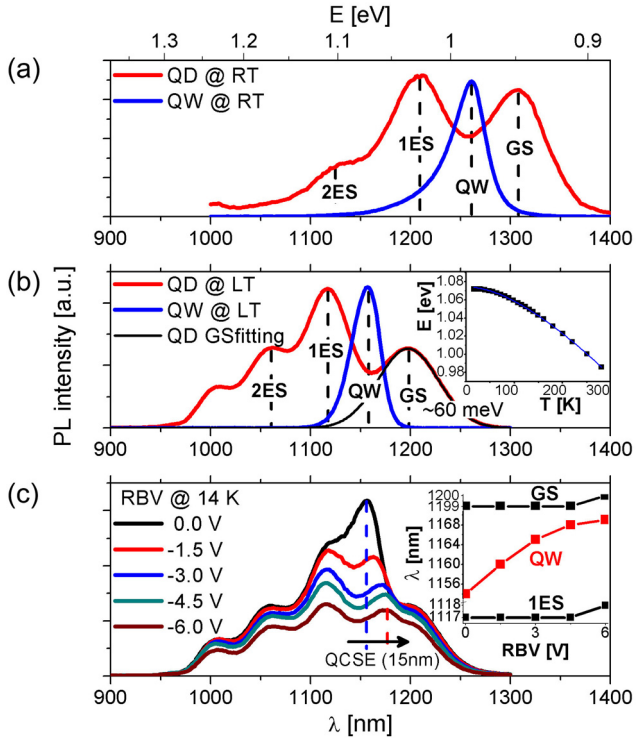

FIG. 2. PL spectra of separate InAs QD and GINA QW intrinsic samples at (a) room temperature and (b) at 14 K. The temperature dependent PL peak energy emission proving minimal carrier localization effect in the intrinsic QW sample is shown in inset. (c) Low (14 K) temperature reverse bias voltage (0 V-6 V) dependent PL of hybrid QD-QW showing the QCSE within the QW. The inset shows the fitted QW peak wavelength as a function of bias and its redshift of 15 nm, while the QDs indicate no shift in wavelength.

underneath the six QD layers. Indeed the nitrogen incorporation and the low growth temperature, necessary to keep bi-dimensional growth, result in a high NRR density. By cooling the p-i-n sample down to 14 K, the NRR centers could be inhibited and the QW emission clearly visible. The low temperature PL spectra for the QW sample and QD sample are shown in [Fig. 2(b)], which helps to identify all the features in the p-i-n sample. Compared to the RT spectra, for both QW and QDs the emissions are shifted by approximately 100 nm (90 meV) to the blue. As the GINA QW material is well known for its strong carrier localization manifesting itself by an S-shaped behaviour of the temperature dependent emission energy,[16–18] we performed a set of temperature-dependent (14 K–280 K) PL measurements at different excitation powers (30 μW – 30 mW). By examining both the excitation power variation and the energy difference $E_{loc}(T) = E(T) - E_{PL}(T)$ (where E(T) is the high-temperature range fit using the Varshni model with $\alpha = 6.7 \pm 0.4 \times 10^{-4}$ eV K^{-1} and $\beta = 335 \pm 20$ K and $E_{PL}(T)$ is the PL peak energy at low excitation powers[18]), the maximum carrier localization energy was estimated to be around 3-4 meV for the intrinsic QW sample [Fig. 2(b) inset]. For the hybrid QD-QW p-i-n sample, the carrier localization effect was further minimized and no measurable difference of the PL peak energy under different excitation powers was observed. This is a consequence of three effects. First the nitrogen concentration is very low (1.5%). Second the carrier localization energy decreases with increasing indium (0%-30%) concentration,[19] and in our case the indium concentration is around 35%. Third, and lastly, the GINA QW inside the hybrid p-i-n sample underwent in-situ annealing during the top p-doped cladding layer growth at 600 °C. This leads to the atomic reorganization and a much more even nitrogen distribution thereby minimizing nitrogen clustering and leading to a crystal quality improvement.[20] All these effects suggest that one should neglect the carrier localization phenomena inside the QW of the hybrid p-i-n sample.

The spectral evolution of the hybrid structure as a function of the reverse bias voltage (RBV) measured at 14 K is shown in [Fig. 2(c)]. The maximum RBV of −6 V, together with built-in voltage of 0.8 V, corresponds to total field strength of 110 kV/cm. For RBV ranging from −6 V to 0 V, the integrated PL intensity had a linear relationship with applied bias. From a multi-peak fitting procedure (where all the QD states were fitted by Gaussian curves, whilst the QW peak was fitted by a single asymmetrical function) the QW contribution has been extracted and is reported in the inset [Fig. 2(c) inset]. As can be seen, the QW peak position is red-shifted by about 15 nm (13 meV) at maximum RBV, while the QD states (GS, 1ES) were comparatively unaffected. This behaviour demonstrates the ability to change the mutual detuning of QW and QD energy levels, through their very different QCSE shifts.

For operation in optical modulator and saturable absorber devices, the absorption recovery time is a crucial parameter. To study the carrier dynamics, we performed a set of time-resolved photoluminescence (TRPL) experiments for the hybrid p-i-n and GINA QW sample (for thermal properties measurement). With its higher saturation fluence and

expected faster recovery times, we mainly focused on the dynamics of the GINA QW, but the QD signal was analyzed as well. To pump the structure, a 300 fs pulsewidth, mode-locked Ti:Sapphire laser tuned to 1015 nm was used. At this excitation wavelength and with a low (14 K) sample temperature, the photo-generation of electron-hole pairs is avoided both in the GaAs barriers and in the InGaAs wetting layers (WLs), thus preventing the creation of a carrier reservoir. The highest energy state excited is the second excited state inside the QD. Specific care was also taken to minimize the generation of higher energy carriers through the two-photon absorption process. The GINA QW ground state electron-hole (e1-hh1) PL lifetime depends on four relaxation/escape mechanisms: radiative recombination, τ_{rad}; non-radiative recombination through NRR centers, τ_{nonrad}; thermionic emission, τ_{th}; and field induced tunnelling, τ_{tun}. As was mentioned earlier, the 125 nm GaAs spacer prevents any carrier relaxation/tunnelling into the QD ground state from the QW and from the QD excited states into the QW. Thus, the only other mechanism acting to decrease the QW PL decay rate would be the electron-hole pair generation by absorption of photons originating from radiative recombination in the higher QD states (i.e., 2ES and 1ES) inside the IAR. However, this only makes a minor contribution and so can be neglected. Therefore, the GINA QW can be considered to be an isolated system and the total QW PL decay rate can be expressed as

$$\tau^{-1} = \tau_{rad}^{-1} + \tau_{norad}^{-1} + \tau_{th}^{-1} + \tau_{tun}^{-1}. \quad (1)$$

In order to better understand the dynamics within the QW region and the significance of the individual contributions, two specific measurements were carried out. The first experiment was TRPL as a function of RBV performed at 14 K, where both thermionic emission and NRR processes are significantly suppressed, and thus the dominant contribution is from field induced tunnelling. External biases, varying from 0.0 V down to −8.0 V, were applied. In the streak images [Fig. 3(a)], we can observe not only the QW redshift as expected from the PL measurement, but also dynamical features indicative of radiative recombination. To quantify the decay times of the QW in the hybrid structure, we have sectioned the streak images along its peak wavelength (denoted by dashed lines) and obtain the decay traces [Fig. 3(b)]. After deconvolving the measured data with the system response [Fig. 3(b) dashed line], we proceeded with fitting. The QD GS decay times were extracted at its peak wavelength (1200 nm) and the voltage insensitive value of around 1400 ps was found and is in the typical range of InAs DWELL systems measured at low temperature. As the QD GS emission, with its 60 meV width [Fig. 2(b) QD GS fitting], overlaps the emission from the QW (especially at higher RBV), we have fitted the decay traces with a double exponential function with a fast component (voltage sensitive) belonging to the QW emission and a slow component (voltage insensitive) to the QD GS blue tail. With increasing RBV, the photo-generated carriers effectively tunnel through the GaAs barrier into the external circuitry and decay times shorten. The extracted QW decay times τ_{QW} [Fig. 3(b) inset] exponentially follow the applied RBV with the QW decay time varying from 150 ps (0.0 V) down to 74 ps (−8.0 V). The slow component decay times τ_{QD} were around 1400 ps, which is in agreement with the QD GS decay times extracted at 1200 nm discussed above.

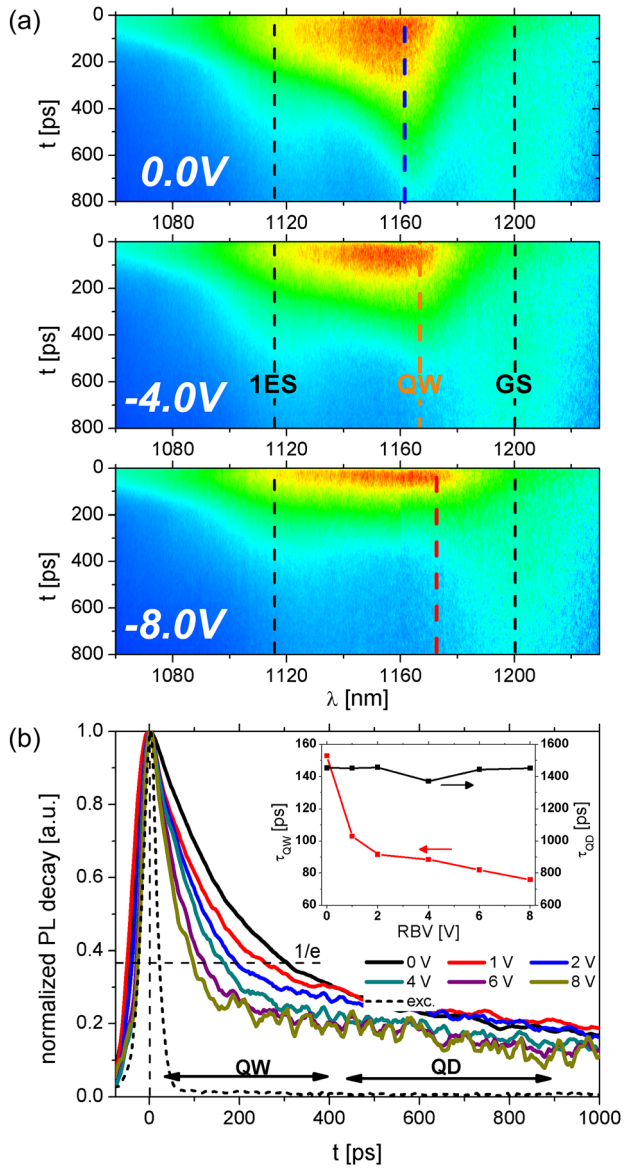

FIG. 3. The TRPL streak images at 0.0 V, −4.0 V, and −8.0 V showing both wavelength positions and temporal dynamics of the QD and QW states. (b) RBV (0.0 V-8.0 V) dependent PL decay curves of GINA QW revealing its shortening due to the heavy-hole tunnelling at low 14 K temperature. Inset shows that GINA QW extracted decay times exponentially follow the RBV applied, i.e., from 150 ps at 0.0 V down to 74 ps at −8.0 V, while QD GS decay times are unaffected with constant value of 1400 ps.

In the second experiment, the NRR and thermal escape contributions on the QW PL decay time have been determined. We measured the intrinsic QW structure (no external voltage applied) PL decay under different temperatures ranging from 13 K up to 290 K under the same excitation conditions as above [Fig. 4]. The impact of temperature increase was twofold. First, the thermal activation of the NRRs induces a progressive change of the QW PL decay curve shape from a convex line (13 K) to a straight line (160 K) in semi-log scale.[21] As the temperature increases further and reaches

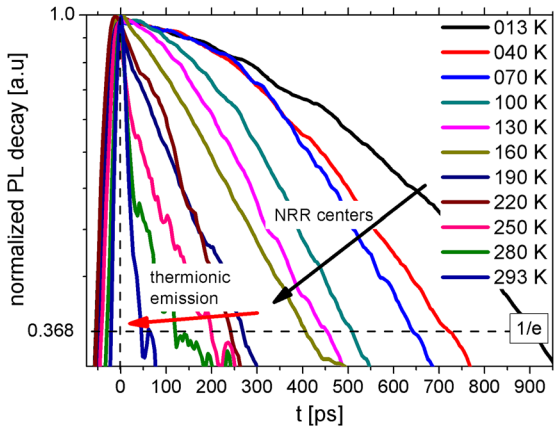

FIG. 4. Temperature dependent (13-290 K) TRPL measurement of GINA QW showing first the thermal activation of NRR centers responsible for radiative recombination decay time shortening and further shortening due to the hole leakage (thermionic emission) at elevated (>190 K) temperature.

190 K, the carrier thermal energy k_bT is approximately equal to half of the hh-barrier offset thus leading to thermionic emission.[22] This hole leakage leads to further shortening in PL decay times down to 50 ps at 290 K. Thus at room temperature, together with using external bias to induce tunnelling, we can easily expect PL lifetimes shorter than 30 ps, which become suitable for high speed direct modulation.

In summary, we have shown the properties of a GINA QW embedded in a hybrid p-i-n structure together with six stacked InAs/InGaAs QDs layers. As QDs show low sensitivity to the applied voltage in terms of QCSE shift and carrier dynamics, and low absorption due to their limited density of states, we have shown the GINA QWs potential of providing controlled variable absorption with fast recovery working at 1300 nm. This hybrid QD-QW material could be utilized as an effective Electro-Absorption Modulator (EAM) and/or saturable absorber in integrated EML devices or modern reconfigurable multisection device. The combination of nonradiative recombination, thermionic emission, and voltage induced tunnelling gives rapid PL decay at room temperature and thus the potential for high speed (>20 Gbit/s) operation. Moreover, this type of structure offers number of parameters that can be optimized or tuned. For instance, the intrinsic region could be narrowed to increase the strength of the applied electric field on the Stark shift, and thus reducing device power consumption. Further, bandgap engineering in terms of composition, width and also QWs stacking (double QW) could enhance device performances.

This research was supported by Science Foundation Ireland through the PiFAS Grant No. 07/SRC/I1173.

[1]Y. Arakawa and H. Sakaki, Appl. Phys. Lett. **40**(11), 939 (1982).
[2]S. Freisem, G. Ozgur, K. Shavritranuruk, H. Chen, and D. G. Deppe, Electron. Lett. **44**(11), 679 (2008).
[3]S. S. Mikhrin, A. R. Kovsh, I. L. Krestnikov, A. V. Kozhukhov, D. A. Livshits, N. N. Ledentsov, Yu. M. Shernyakov, I. I. Novikov, M. V. Maximov, V. M. Ustinov, and Zh. I. Alferov, Semicond. Sci. Technol. **20**(5), 340 (2005).
[4]A. Capua, L. Rozenfeld, V. Mikhelashvili, G. Eisenstein, M. Kuntz, M. Laemmlin, and D. Bimberg, Opt. Express **15**(9), 5388 (2007).
[5]E. U. Rafailov, M. A. Cataluna, W. Sibbett, N. D. Il'Æinskaya, Yu. M. Zadiranov, A. E. Zhukov, V. M. Ustinov, D. A. Livshits, A. R. Kovsh, and N. N. Ledentsov, Appl. Phys. Lett. **87**(8), 081107 (2005).
[6]M. G. Thompson, A. R. Rae, M. Xia, R. V. Penty, and I. H. White, IEEE J. Sel. Top. Quantum Electron. **15**(3), 661 (2009).
[7]C. Y. Ngo, S. F. Yoon, W. K. Loke, Q. Cao, D. R. Lim, V. Wong, Y. K. Sim, and S. J. Chua, Appl. Phys. Lett. **94**(14), 143108 (2009).
[8]P. Bhattacharya and S. Ghosh, Appl. Phys. Lett. **80**(19), 3482 (2002).
[9]W. Rudno-Rudzinski, G. Sek, K. Ryczko, M. Syperek, J. Misiewicz, E. S. Semenova, A. Lemaitre, and A. Ramdane, Appl. Phys. Lett. **94**(17), 171906 (2009).
[10]M. Kondow, K. Uomi, A. Niwa, S. Watahaki, Y. Yazawa, and M. Okai, Jpn. J. Appl. Phys. **35**, 1273 (1996).
[11]J. W. Ferguson, P. Blood, P. M. Smowton, H. Bae, T. Sarmiento, J. S. Harris, N. Tansu, and L. J. Mawst, IEEE J. Quantum Electron. **47**(6), 870 (2011).
[12]V. Lordi, H. B. Yuen, S. R. Bank, J. S. Harris, Appl. Phys. Lett. **85**(6), 902 (2004).
[13]A. Ramdane, F. Devaux, N. Souli, D. Delprat, and A. Ougazzaden, IEEE J. Sel. Top. Quantum Electron. **2**(2), 326 (1996).
[14]Y. C. Xin, Y. Li, Vassilios Kovanis, A. L. Gray, L. Zhang, and L. F. Lester, Opt. Express **15**(12), 7623 (2007).
[15]H. Y. Liu, I. R. Sellers, M. Gutiérrez, K. M. Groom, W. M. Soong, M. Hopkinson, J. P. R. David, R. Beanland, T. J. Badcock, D. J. Mowbray, and M. S. Skolnick, J. Appl. Phys. **96**(4), 1988 (2004).
[16]S. Mazzucato, R. J. Potter, A. Erol, N. Balkan, P. R. Chalker, T. B. Joyce, T. J. Bullough, X. Marie, H. Carrere, E. Bedel, G. Lacoste, A. Arnoult, and C. Fontaine, Physica E (Amsterdam) **17**, 242 (2003).
[17]X. Liang, D. Jiang, B. Sun, L. Bian, Z. Pan, L. Li, and R. Wu, J. Cryst. Growth **243**(2), 261 (2002).
[18]M. A. Pinault and E. Tournié, Appl. Phys. Lett. **78**(11), 1562 (2001).
[19]Q. X. Zhao, S. M. Wang, Y. Q. Wei, M. Sadeghi, A. Larsson, and M. Willander, Phys. Lett. A **341**, 297 (2005).
[20]H. Zhao, Y. Q. Xu, H. Q. Ni, S. Y. Zhang, Q. Han, Y. Du, X. H. Yang, R. H. Wu, and Z. C. Niu, Semicond. Sci. Technol. **21**(3), 279 (2006).
[21]Z. Sun, Z. Y. Xu, X. D. Yang, B. Q. Sun, Y. Ji, S. Y. Zhang, H. Q. Ni, and Z. C. Niu, Appl. Phys. Lett. **88**(1), 011912 (2006).
[22]M. Hugues, B. Damilano, J.-Y. Duboz, and J. Massies, Phys. Rev. B **75**(11), 115337 (2007).